0026-895X/97/050886-10$3.00/0

MOLECULAR PHARMACOLOGY, **52:**886–895 (1997).

Potentiation and Inhibition of Neuronal Nicotinic Receptors by Atropine: Competitive and Noncompetitive Effects

RUUD ZWART and HENK P. M. VIJVERBERG

Research Institute of Toxicology, Utrecht University, NL-3508 TD Utrecht, The Netherlands

Received January 22, 1997; Accepted July 16, 1997

SUMMARY

Atropine, the classic muscarinic receptor antagonist, inhibits ion currents mediated by neuronal nicotinic acetylcholine receptors expressed in *Xenopus laevis* oocytes. At the holding potential of −80 mV, 1 μM atropine inhibits 1 mM acetylcholine-induced inward currents mediated by rat α2β2, α2β4, α3β2, α3β4, α4β2, α4β4, and α7 nicotinic receptors by 12–56%. Inward currents induced with a low agonist concentration are equally inhibited (α3β2, α3β4), less inhibited (α2β4, α7), or potentiated (α4β2, α4β4) by 1 μM atropine. Effects on the more sensitive α4β4 nicotinic receptors were investigated in detail by systematic variation of acetylcholine and atropine concentrations and of membrane potential. At high agonist concentration, atropine inhibits α4β4 nicotinic receptor-mediated ion current in a noncompetitive, voltage-dependent way with IC_{50} values of 655 nM at −80 mV and of 4.5 μM at −40 mV. At low agonist concentration, 1 μM atropine potentiates α4β4 nicotinic receptor-mediated ion current. This potentiating effect is surmounted by high concentrations of acetylcholine, indicating a competitive interaction of atropine with the nicotinic receptor, and potentiation is also reversed at high atropine concentrations. Steady state effects of acetylcholine and atropine are accounted for by a model for combined receptor occupation and channel block, in which atropine acts on two distinct sites. The first site is associated with noncompetitive ion channel block. The second site is associated with competitive potentiation, which appears to occur when the agonist recognition sites of the receptor are occupied by acetylcholine and atropine. The apparent affinity of atropine for the agonist recognition sites of the α4β4 nicotinic acetylcholine receptor is estimated to be 29.9 μM.

The neurotransmitter ACh signals through two distinct types of receptors: nAChRs and mAChRs. These two classes of receptors for ACh were already distinguished pharmacologically by Sir Henry Dale in 1914 (1) on the basis of the resemblance of ACh effects with those of naturally occurring plant alkaloids. mAChRs are activated selectively by muscarine and blocked by atropine, and nAChRs are activated selectively by nicotine and blocked by curare (2, 3). This classification found support from biochemical and electrophysiological data, which showed that nicotinic and muscarinic receptors are functionally distinct entities. Molecular cloning has further demonstrated that the primary structure of nicotinic and muscarinic receptor proteins falls into two different gene families, the ligand-gated ion channels and G protein-coupled receptors, respectively (4–6).

Atropine is still widely used to selectively antagonize mAChRs. mAChRs are sensitive to atropine, with IC_{50} values in the nanomolar concentration range (see Ref. 7). At these concentrations, atropine is believed to have few or no side effects on nAChRs because very high (near-millimolar) concentrations of atropine are required to cause any degree of inhibition of the effects of ACh at end-plate-type nAChRs and neuronal-type nAChRs in autonomic ganglia (8–10).

In recent years, however, a multiplicity of neuronal nAChRs have been identified (for reviews, see Refs. 6 and 11). Known subunits of neuronal nAChRs (α2–9 and β2–4) combine in various compositions to generate pentameric complexes with different functional and pharmacological characteristics. Atropine has been reported to inhibit several types of ligand-gated ion channels. Ion currents mediated by homo-oligomeric α7, α8, and α9 nAChRs as well as the homo-oligomeric serotonin type 3 receptor are inhibited with IC_{50} values in the range of 0.4–7 μM atropine (12–14). Atropine displaces α-bungarotoxin from homo-oligomeric nAChRs, and noncompetitive interaction of atropine with these receptors has also been suggested (12). However, the mechanism of the inhibition of the nAChR-mediated ion currents by atropine is unresolved. Effects of atropine on heteromeric neuronal nAChRs, which differ from the homo-oligomeric nAChRs by their insensitivity to α-bungarotoxin (see Refs. 11 and 15), have not been reported.

In this study, we investigated and compared the effects of atropine on various subunit combinations of nAChRs ex-

This work was supported by Netherlands Organization for Scientific Research (NWO) Grant 903–42-011.

ABBREVIATIONS: ACh, acetylcholine; mAChR, muscarinic acetylcholine receptor; nAChR, nicotinic acetylcholine receptor; HEPES, 4-(2-hydroxyethyl)-1-piperazineethanesulfonic acid.

pressed in *Xenopus laevis* oocytes, and the mechanism of atropine action was investigated in detail on the $\alpha4\beta4$ nAChR. Part of this work has appeared in abstract form (16).

Experimental Procedures

Materials. *X. laevis* were bred and kept in the Hubrecht Laboratory (Utrecht, The Netherlands). Acetylcholine chloride, (−)-nicotine bitartrate, gentamicin, 3-amino-benzoic acid ethyl ester, and collagenase type I were from Sigma Chemical (St. Louis, MO), and atropine sulfate was from Fluka (Buchs, Switzerland). All other salts and HEPES were from Merck (Darmstadt, Germany). cDNAs of nicotinic receptor subunits ligated into the pSM plasmid vector containing the SV40 viral promotor were a kind gift from Dr. J. Patrick (Baylor College of Medicine, Houston, TX).

Expression in oocytes. Mature female specimen of *X. laevis* were anesthetized by submersion in 0.1% 3-aminobenzoic acid ethyl ester and ovarian lobes were surgically removed. Oocytes were defolliculated manually after treatment with collagenase type I (1.5 mg/ml calcium-free Barth's solution) for 1.5 hr at room temperature. Plasmids coding for α and β subunits of neuronal nAChRs, dissolved in distilled water at a 1:1 molar ratio, were coinjected into the nuclei of stages V and VI oocytes within 8 hr after harvesting, using a Drummond microinjector. Approximately 1 ng of each plasmid containing α and β cDNA (2 ng for $\alpha7$) was injected in a total injection volume of 10–15 nl/oocyte. After injection oocytes were incubated at 19° in modified Barth's solution containing 88 mM NaCl, 1 mM KCl, 2.4 mM $NaHCO_3$, 0.3 mM $Ca(NO_3)_2$, 0.41 mM $CaCl_2$, 0.82 mM $MgSO_4$, 15 mM HEPES, and 10 μg/ml gentamicin (pH 7.6 with NaOH). Experiments were performed on oocytes after 2–5 days of incubation.

Electrophysiology and data analysis. Oocytes were voltage-clamped using two microelectrodes (0.5–2.5 MΩ) filled with 3 M KCl and a custom-built voltage clamp amplifier with high-voltage output stage according to the methods described by Stühmer (17). The external saline was clamped at ground potential by means of a virtual ground circuit using an Ag/AgCl reference electrode and a Pt/Pt-black current passing electrode. Membrane current was measured with a current-to-voltage converter incorporated in the virtual ground circuit. The membrane potential was held at −80 mV, unless otherwise indicated. All experiments were performed at room temperature (22–24°).

Oocytes were placed in a silicon tube (i.d. 3 mm), which was continuously perfused with saline solution (115 mM NaCl, 2.5 mM KCl, 1 mM $CaCl_2$, 10 mM HEPES, pH 7.2, with NaOH) at a rate of ~20 ml/min. Aliquots of freshly prepared, concentrated stock solutions of atropine sulfate and acetylcholine chloride in distilled water were added to the saline immediately before the experiments. Drugs were applied by switching between control and drug-containing saline using a servomotor-operated valve. Agonist applications were alternated by 5 min of superfusion with agonist-free saline to allow the receptors to recover completely from desensitization. Membrane currents were low-pass filtered (eight-pole Bessel; −3 dB at 0.3 kHz), digitized (12 bits; 1024 samples/record), and stored on disk for off-line computer analysis. Data are expressed as mean ± standard deviation. Results are compared using a two-tailed Student's *t* test. Curve fitting was performed by a nonlinear least-squares algorithm (18).

Results

Atropine inhibits neuronal nAChRs. Superfusion of voltage-clamped oocytes expressing different subunit combinations of neuronal nAChRs with 1 mM ACh evoked typical inward ligand-gated ion currents. The kinetics of the inward currents varied for the different subunit combinations and with some subtypes of nAChR tail currents were observed on washout of the high concentration of the agonist (Fig. 1). To

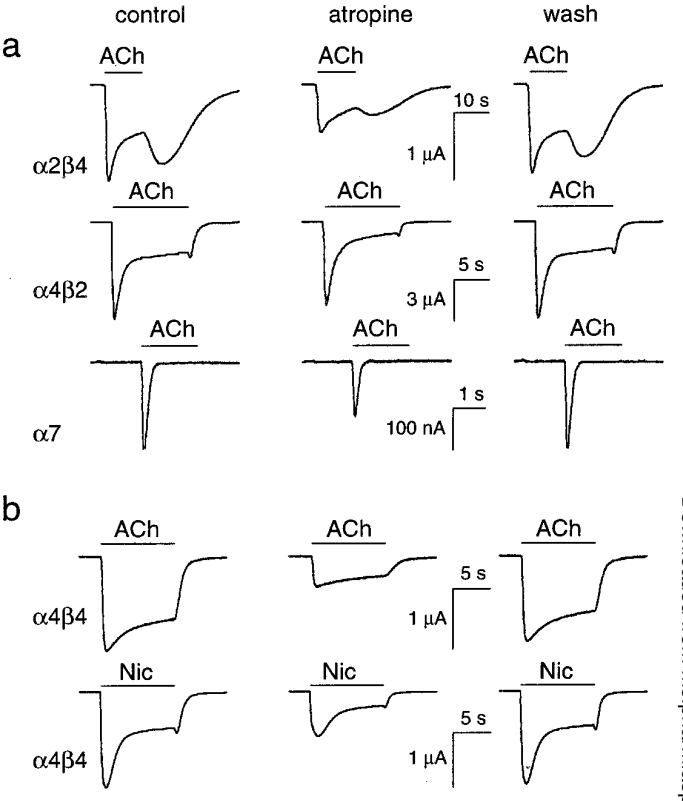

Fig. 1. Atropine inhibits neuronal nAChR-mediated ion currents. A, Inhibition of 1 mM ACh-induced ion currents in oocytes expressing $\alpha2\beta4$, $\alpha4\beta2$, and $\alpha7$ nAChRs. *Left*, control ion currents evoked by ACh. *Center*, ion currents evoked by ACh in the presence of 1 μM atropine. *Right*, recovery from inhibition after 4 min of washing. *Horizontal bars*, periods of superfusion with ACh. The tail currents that are observed on removal of ACh in oocytes expressing $\alpha2\beta4$ and $\alpha4\beta2$ reflect the unblocking of ion channels that were blocked by the high concentration of ACh. B, 1 μM atropine blocks 100 μM ACh- and 100 μM nicotine-induced ion currents in oocytes expressing $\alpha4\beta4$ nAChRs to the same extent. Experimental conditions are the same as for A.

investigate the effects of atropine, oocytes were superfused with saline-containing atropine for ≥4 min, inward currents were evoked by switching the superfusate to saline-containing ACh and the same concentration of atropine, and subsequently, the agonist was washed out by switching back to atropine-containing saline. For all subunit combinations tested, the peak amplitude of the inward current evoked by 1 mM ACh was reduced in the presence of 1 μM atropine. Examples of the inhibitory effects of atropine are shown in Fig. 1A. The degree of inhibition by atropine varied for the different combinations of nAChR subunits. The results for the reduction in the peak amplitude of 1 mM ACh-induced inward currents by 1 μM atropine are summarized in Table 1 for the subtypes of nAChRs that were tested. Atropine in the concentration range of 1 μM to 1 mM did not induce any detectable change in membrane holding current on itself.

A number of experiments were performed to exclude the possibility that atropine exerted its effects on ACh-induced ion currents via endogenous mAChRs, which are supposed to be present in *X. laevis* oocytes (19, 20). In oocytes expressing $\alpha4\beta4$ nAChR, the ion current evoked by the selective nAChR agonist (−)-nicotine was inhibited by 1 μM atropine to 41.7 ± 4.5% (three oocytes), and the ACh-induced ion current was inhibited to 41.3 ± 5.0% (four oocytes). Inhibition of the

TABLE 1

Effects of 1 μM atropine on the peak amplitude of near-maximum amplitude ion currents induced by 1 mM ACh and on small (<10% of I_{max}) ion currents induced by 1 μM ACh for various subunit combinations of neuronal nAChRs

All currents were recorded at −80 mV, and the percent response was obtained by normalizing the peak amplitude in the presence of atropine to the peak amplitude of control responses evoked by the same concentration of ACh. Values represent mean ± standard deviation measured for the number of oocytes (*n*). For each subunit combination, results were obtained from oocytes of three to five frogs (*left*) and of two frogs (*right*). All effects of atropine were statistically significant with respect to control values (paired *t* tests; $p < 0.007$).

nAChR	1 mM ACh response	1 μM ACh response	p^a
	%		
α2β2	85.9 ± 7.8 (6)	N.D.[b]	
α2β4	51.0 ± 3.0 (6)	93.5 ± 2.8 (6)	<0.001
α3β2	85.9 ± 3.7 (10)	91.0 ± 4.6 (6)	0.03
α3β4	87.5 ± 4.7 (6)	88.3 ± 4.3 (6)[c]	0.76
α4β2	74.1 ± 7.2 (7)	140.5 ± 4.9 (6)	<0.001
α4β4	43.5 ± 4.5 (6)	170.3 ± 10.2 (6)	<0.001
α7	53.3 ± 4.8 (6)	81.9 ± 3.5 (4)[c]	<0.001

[a] Student's *t* test probability of the hypothesis that the effect of atropine on responses evoked by high agonist concentration (*left* column) equals the effect on responses evoked by low agonist concentration (*right* column).
[b] Not determined because large numbers of receptors were not expressed.
[c] Inward currents induced with 10 μM ACh.

ACh-induced ion current does not differ significantly from inhibition of nicotine-induced current by atropine (*t* test: $p = 0.91$; Fig. 1B). This indicates that block of putative endogenous mAChRs in the oocytes did not play a role in the atropine effects observed. In addition, at least three uninjected oocytes from every batch of oocytes used were tested for responses to ACh. In these oocytes, as well as in oocytes that had been injected with nAChR subunit cDNAs but did not express functional nAChRs, changes in membrane current were never induced by superfusion with 100 μM ACh at the holding potentials of −80 and −20 mV. The results indicate that endogenous mAChRs, if present in the oocytes used in this study, did not mediate electrophysiological responses and did not interfere with nAChR-mediated ion currents. It is concluded that atropine interacts directly with the nAChR. Because the α4β4 nAChR was one of the more sensitive subunit combinations (see Table 1), the mechanism of action of atropine has been investigated in detail in oocytes expressing these receptors.

Mechanism of inhibition of α4β4 nAChR-mediated ion currents by atropine. The concentration-dependent effects of atropine on α4β4 nAChRs were investigated in oocytes superfused with various concentrations of atropine. On the first response to 100 μM ACh in the presence of atropine, which was evoked after ~5 min of superfusion with atropine-containing saline, the inhibitory effect on the peak amplitude of α4β4 nAChR-mediated current had reached a steady level. Examples of inward currents evoked by superfusion of 100 μM ACh in the absence and presence of various concentrations of atropine and the concentration-effect curve for reduction in the peak amplitude of the α4β4 nAChR-mediated inward current by atropine are shown in Fig. 2A. The inhibition curve fitted to the data yielded estimates for the IC_{50} values of atropine of 655 ± 35 nM and for the slope factor of −0.92 ± 0.04. The inhibitory effects of atropine were reversed completely within 5 min of washing, which was also the interval maintained between subsequent agonist applications (Fig. 1).

Concentration-effect curves of ACh were obtained from oocytes expressing α4β4 nAChRs in the absence and presence of atropine. An example of responses evoked by superfusion of 1–1000 μM ACh in the absence and presence of 1 μM atropine recorded from a single oocyte is shown in Fig. 2B. For three oocytes, peak inward current amplitudes were normalized to those of control inward currents evoked by 1 mM ACh in the same oocyte and data obtained in the absence and in the presence of 1 μM atropine were plotted against agonist concentration. Fitting concentration-effect curves to the data obtained from these experiments yielded estimates of EC_{50}, slope factor, and E_{max} of 13.8 ± 0.7 μM ACh, 1.2 ± 0.1, and 110 ± 2% in the control situation and 8.5 ± 0.8 μM ACh, 1.0 ± 0.1, and 51 ± 1%, respectively, in the presence of 1 μM atropine (Fig. 2B). The data measured at the highest agonist concentration were excluded from the curve-fitting procedure because this high concentration of ACh caused a reduction of the peak amplitude of the ACh-induced inward current. The concentration-effect curves show that in the presence of 1 μM atropine, the inward currents induced by concentrations of >10 μM ACh were inhibited to the same extent. At the agonist concentrations of ≤ 3 μM, no inhibition of ACh-induced current responses by 1 μM atropine was observed. Instead, at 1 μM ACh, the amplitude of the inward current was enhanced in the presence of atropine to 189 ± 35% (three oocytes) of the control values. The effect of atropine on the concentration-effect curve of ACh (i.e., a marked reduction in E_{max} and no large shift in EC_{50} value) indicates that atropine exerts its inhibition via a noncompetitive mechanism. A small but significant change in the EC_{50} value and slope factor of the concentration-effect curve for ACh is most likely due to the potentiation of α4β4 nAChR-mediated ion currents by atropine at low agonist concentration. This potentiating effect of atropine has been investigated separately (see below).

Effects of membrane potential were investigated to obtain an indication of the mechanism underlying the inhibitory effect of atropine. In the absence of extracellular atropine, the amplitude of the 100 μM ACh-induced current decreased at less negative holding potentials (Fig. 3A), and ACh-induced ion currents were not observed on application of 100 μM ACh at positive holding potentials (not shown). In the presence of atropine, the ACh-induced inward current was markedly reduced at strongly hyperpolarized membrane potentials, and smaller inhibitory effects were observed at more depolarized membrane potentials. The current-voltage relationships of 100 μM ACh-induced ion currents in the absence and presence of 1 and 10 μM atropine are depicted in Fig. 3A. These results demonstrate that inhibition of nAChR-mediated ion currents by atropine is voltage dependent, suggesting that atropine acts by blocking the nAChR channel. Further evidence for open channel block by atropine came from experiments in which atropine was coapplied with ACh (Fig. 3B). The application of 10 μM atropine did not induce a change in membrane holding current on its own. The application of 10 μM ACh to oocytes expressing α4β4 nAChRs and voltage-clamped at −100 mV induced a virtually nondesensitizing inward current. On removal of ACh, the current returned to the base-line level. The coapplication of 10 μM ACh with 10 μM atropine induced an inward current that was much smaller than the current elicited by ACh alone. In addition, the current evoked by the coapplication decayed toward a steady level, and a transient increase in membrane

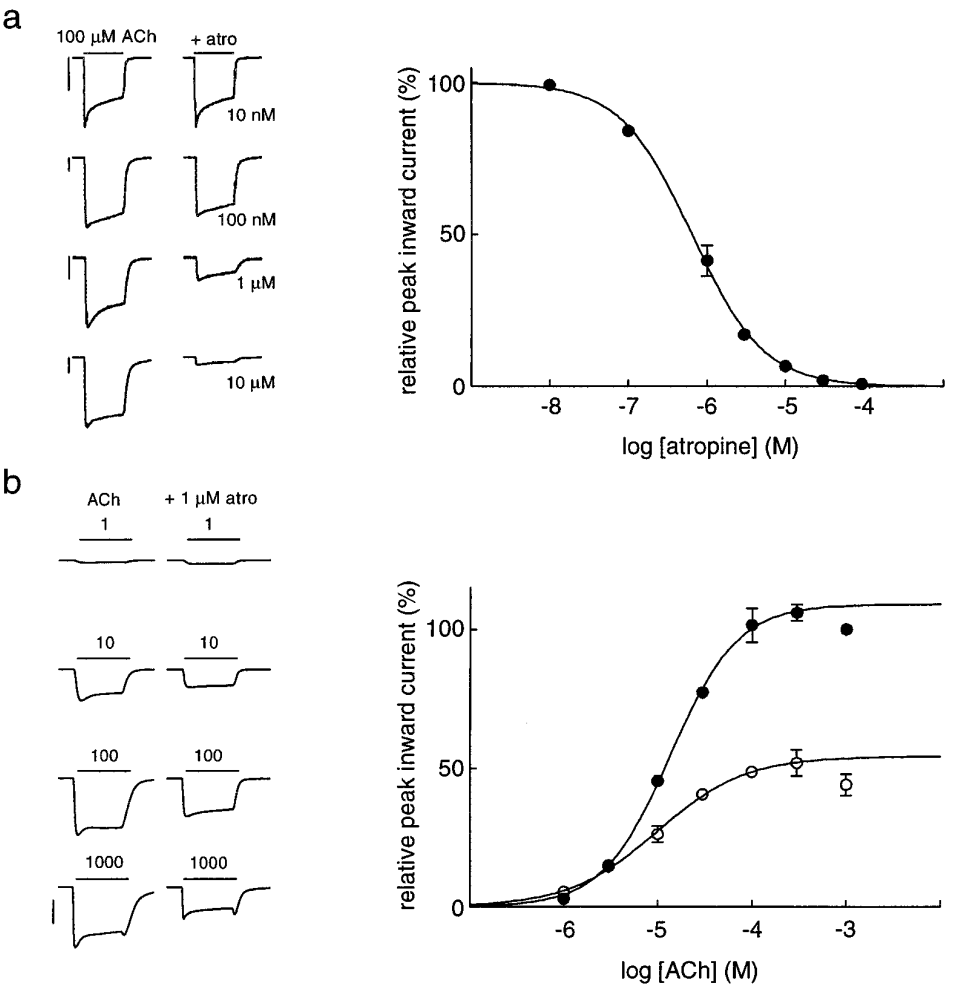

Fig. 2. Atropine inhibits $\alpha4\beta4$ nAChR-mediated ion current in a noncompetitive manner. A, *left*, inward currents evoked by superfusion of 100 μM ACh for 10-sec periods (*bars*) under control conditions and in the presence of various concentrations of atropine. Each ACh-induced current was obtained from a different oocyte. *Right*, concentration-effect curve for the inhibitory effect of atropine. *Data points*, mean ± standard deviation values (*bars*) for three to six oocytes (except one oocyte for 3, 30, and 100 μM). At 0.01, 0.1, and 10 μM atropine, the mean ± standard deviation value is smaller than the symbol. *Line*, curve fitted according to the equation: $E = 100/\{1 + (IC_{50}/[\text{atropine}])^n\}$. Estimates for IC_{50} value and n are 655 ± 35 nM and −0.92 ± 0.04, respectively. B, *left*, inward currents evoked in a single oocyte by superfusion of 1, 10, 100, and 1000 μM ACh for 10-sec periods (*bars*) under control conditions and in the presence of 1 μM atropine. *Right*, concentration-effect curves of ACh in the absence (●) and presence (○) of 1 μM atropine. *Data points*, mean ± standard deviation values for three oocytes. The absence of error bars indicates that the mean ± standard deviation is smaller than the symbol. All current amplitudes were normalized to that of control, 1 mM ACh-induced currents. Concentration-effect curves were fitted according to the equation: $E = E_{max}/\{1 + (EC_{50}/[\text{ACh}])^n\}$. Estimates for E_{max}, EC_{50}, and n are 110 ± 2%, 13.8 ± 0.7 μM ACh, and 1.2 ± 0.1 in the absence of atropine and 51 ± 1%, 8.5 ± 0.8 μM ACh, and 1.0 ± 0.1 in the presence of 1 μM atropine, respectively. Note that the response evoked with 1 μM ACh was potentiated by 1 μM atropine. *Vertical calibration bars* (A and B), 1 μA.

current ("tail current") was observed on removal of ACh and atropine by washing. High concentrations of nAChR agonists also cause an acceleration of current decay and a tail current on removal of the agonist (e.g., see Fig. 1A); these phenomena are generally attributed to the onset and reversal of open channel block (21–26). To determine whether atropine or ACh induced the tail current, an additional response was evoked by coapplication of ACh and atropine, but ACh was removed in the continued presence of atropine (Fig. 3B). The absence of a tail current under these experimental circumstances demonstrates that atropine is the agent causing the tail current. The voltage dependence of the blocking effect of atropine is depicted in Fig. 3C. The data obtained from three oocytes exposed to 10 μM atropine were fitted by a Boltzmann curve for voltage-dependent block, and the current-voltage relationships in the presence of atropine (Fig. 3A) were fitted by the same equation. The IC_{50} values for atropine at 0 mV and for the slope yielding best fit of the data in Fig. 3, A and C, were 21.2 μM and 38.7, respectively. It is concluded that the inhibition of ion current induced by a high concentration of agonist at strongly negative membrane potential is due to noncompetitive ion channel block by atropine.

Potentiation of nAChR-mediated ion currents by atropine. Under the conditions used so far, potentiation by atropine was observed only for the $\alpha4\beta4$ nAChR-mediated ion current evoked by a low concentration of ACh at −80 mV. Under the same experimental conditions, $\alpha4\beta2$ nAChR-mediated ion current was also potentiated, whereas ion currents mediated by other heteromeric subunit combinations were slightly inhibited by 1 μM atropine (Table 1). Table 1 shows that $\alpha4\beta4$ was the more strongly affected subtype of nAChR. Because the inhibition of $\alpha4\beta4$ nAChRs by atropine depends

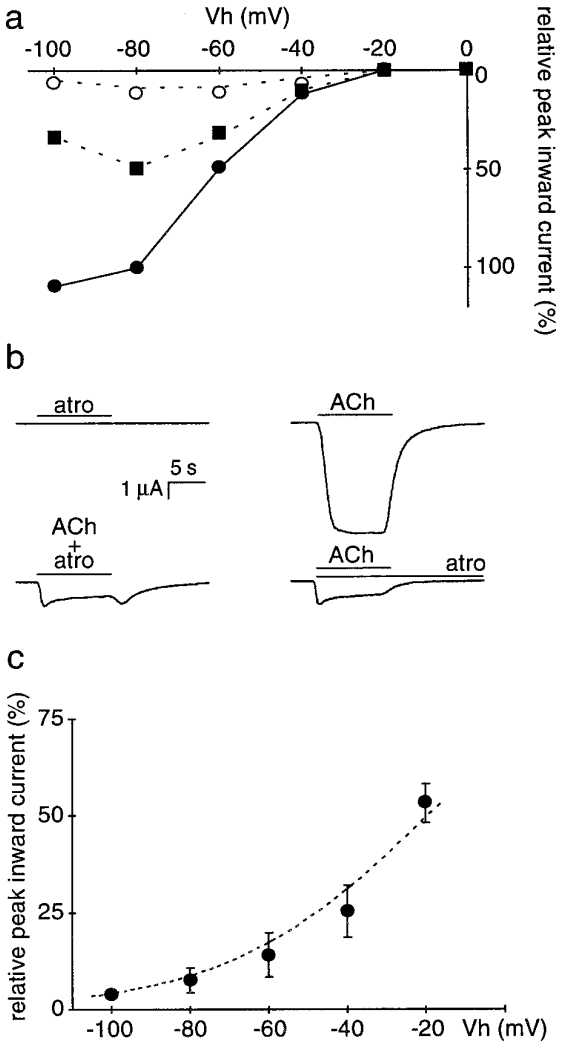

Fig. 3. Voltage dependence of inhibition of $\alpha4\beta4$ nAChR-mediated ion current by atropine. A, Current-voltage relationships of 100 μM ACh-induced ion currents in the absence (●) and presence of 1 μM atropine (■) or 10 μM atropine (○). The peak amplitudes of the ACh-induced currents are normalized to those of control ACh-induced ion currents at −80 mV and are plotted against membrane potential. B, Ion currents demonstrating that atropine is the blocking agent. Superfusion with 10 μM atropine does not induce a change in membrane current on its own. Superfusion with 10 μM ACh evokes a large, virtually nondesensitizing inward current. The ion current induced by coapplication of 10 μM ACh and 10 μM atropine is much smaller than that elicited by 10 μM ACh alone. In addition, this current decays toward a steady level; on removal of ACh and atropine, a tail current is observed. When ACh is removed in the continued presence of atropine after coapplication of 10 μM ACh and 10 μM atropine, a tail current is not observed. This demonstrates that the tail current is caused by atropine. All traces in B were recorded from the same oocyte at a holding potential of −100 mV. Horizontal bars, periods of superfusion with agonist and/or atropine. C, Voltage dependence of 10 μM atropine-induced ion channel block of 100 μM ACh-induced current. *Data points*, mean ± standard deviation percentage of response remaining in the presence of atropine in three oocytes. At each membrane potential, the current amplitude was normalized to that of the ACh-induced current recorded in the absence of atropine. A and C, *dashed lines*, predicted curves according to the Boltzmann function: $Y = 100/\{1 + [\text{atropine}]/[IC_{50}^{0mv} \cdot \exp(V_m \cdot \text{slope})]\}$, using the fitted parameters IC_{50}^{0mv} mV = 21.2 μM and slope = 38.7.

on holding potential (Fig. 3), the membrane potential was varied to improve experimental conditions for investigation of the potentiating effect of atropine on $\alpha4\beta4$ nAChRs. This was done for the effect of a relatively high concentration of 10 μM atropine on responses evoked with the low concentration of 1 μM ACh, for which the potentiation was initially observed (see Fig. 2B). Atropine was applied during apparent steady state responses to 1 μM ACh, so the onset and reversal of the effects of atropine could be observed during a single agonist response. Fig. 4, A and B, shows that at membrane potentials in the range of −30 to −70 mV, the ACh-induced ion current is potentiated by 10 μM atropine. The potentiating effect of atropine, relative to the size of ACh-induced ion current, was largest at the more depolarized membrane potential. At more hyperpolarized membrane potentials, the potentiating effect was reduced and became transient, and only inhibition was observed at the holding potential of −100 mV. This indicates that atropine causes a combination of potentiating and blocking effects. At the more negative membrane potentials, the potentiation is counteracted by inhibition that becomes stronger and more rapid. The tail current on washing out of atropine reflects a mixture of reversal of ion channel block and change in the balance between potentiating and inhibitory effects of atropine, which are caused by the rapid dilution of atropine. The complex nature of these tail currents and the rapid kinetics of the current transients at the onset of the effect of atropine at the more negative membrane potentials preclude the use of these parameters to quantify the potentiating effect of atropine. However, the large amplitude of the tail current indicates that potentiation is not suppressed at the more negative membrane potentials. Measurement of the net, steady effects of atropine at the various holding potentials showed that potentiation and inhibition are approximately equal at holding potentials between −80 and −90 mV. Potentiation predominates at more depolarized holding potentials, and inhibition predominates at more hyperpolarized holding potentials (Fig. 4B). Atropine potentiates the ion current induced by the low concentration of 0.3 μM (−)-nicotine similarly to its potentiation of the 1 μM ACh-induced ion current (Fig. 4C). This result confirms that like the inhibitory effect, potentiation is not mediated by mAChR and shows that potentiation may also occur with nicotinic agonists other than ACh.

At the optimized membrane potential of −40 mV, the concentration-effect curve of ACh was determined. The results in Fig. 5A show that the response amplitude was reduced at ACh concentrations of >1 mM, indicating channel block by ACh. The data from three oocytes were fitted by dual concentration-effect curves for activation and block by ACh. The mean EC_{50} value obtained from the fitted curves was 42.2 ± 18.5 μM, the mean slope factor for activation was 1.12 ± 0.29, the mean E_{max} was 103 ± 3%, and the mean IC_{50} was estimated to be 54.7 ± 22 mM with a fixed value of −1 for the slope factor for inhibition. A number of oocytes injected with $\alpha4$ and $\beta4$ cDNAs did not respond to superfusion with 1 mM ACh, indicating that even this high concentration of ACh does not activate other than nAChR-mediated ion current in oocytes. Channel block by atropine at −40 mV was determined from responses evoked by 1 mM ACh. The concentration-effect curve of atropine (Fig. 5B) reflects mainly noncompetitive block at a high ACh concentration. The IC_{50} value of atropine at −40 mV amounts to 4.5 ± 0.6 μM, and the slope factor is −0.96 ± 0.04 (three oocytes). The IC_{50} value estimated from the inhibition curve is close to the value of 4.1 μM

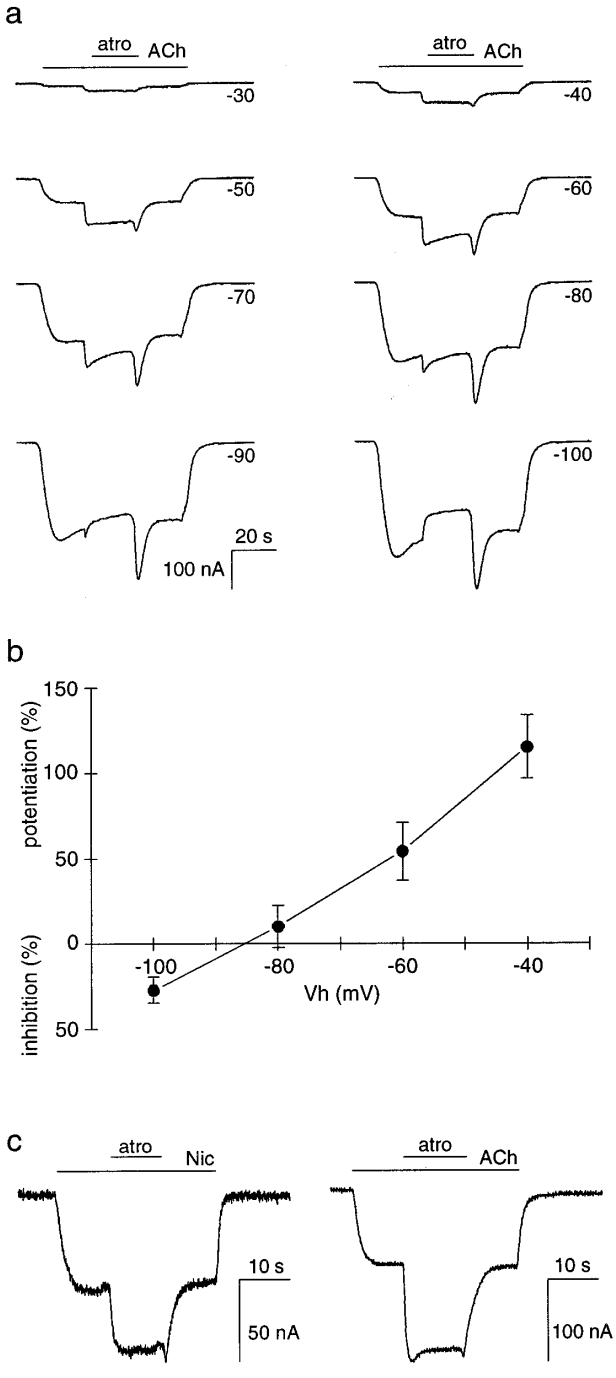

Fig. 4. Effect of membrane potential on the balance between potentiation and inhibition of $\alpha4\beta4$ nAChR-mediated ion current by atropine. A, Effects of 10 μM atropine on 1 μM ACh-induced ion current recorded at membrane potentials ranging from −30 to −100 mV, as indicated. Bars, application of ACh and atropine. The inhibitory effects of atropine are enhanced at more negative membrane potentials, whereas the large tail currents observed on removal of atropine indicate that potentiation occurs at the more negative holding potentials as well. Similar results were obtained from an additional four oocytes. B, Steady state effects of 10 μM atropine on 1 μM ACh-induced ion current measured at different membrane potentials demonstrate that atropine potentiates the ACh-induced inward currents at membrane potentials of ≥ -80 mV. At membrane potentials of ≤ -90 mV, the effect of atropine is reversed into inhibition. *Data points*, mean ± standard deviation (*bars*) values for five oocytes. C, Similar potentiation of 1 μM ACh- and 0.3 μM (−)-nicotine-induced ion currents by 10 μM atropine at −40 mV membrane potential.

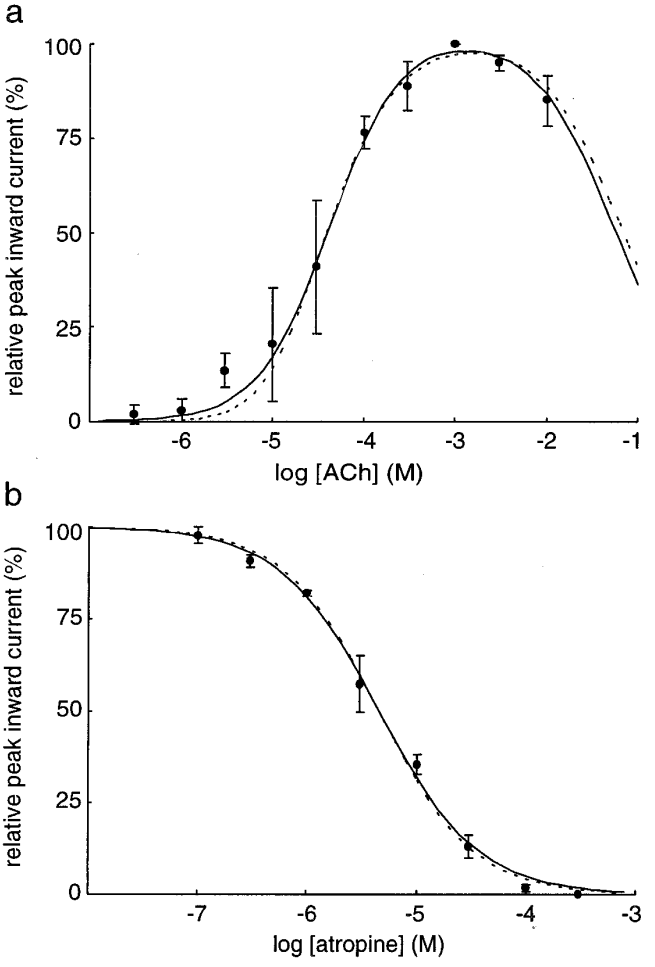

Fig. 5. A, Concentration-effect curve of ACh at −40 mV membrane potential. Peak amplitudes of inward currents evoked by a wide range of ACh concentrations were normalized to the peak amplitude of the 1 mM ACh-induced inward current. Mean ± standard deviation values for three oocytes are plotted against ACh concentration. Concentration-effect curves for activation and inhibition by ACh were fitted to the data of individual experiments according to the equation: $E = E_{max}/\{1 + (EC_{50}/[ACh])^n\}\cdot\{1/(1 + [ACh]/IC_{50})\}$. *Solid line*, mean concentration-effect curve with EC_{50} = 42.2 μM ACh, n = 1.12, E_{max} = 102.8%, and IC_{50} = 54.7 mM (i.e., the calculated mean values of the parameters estimated from the three experiments). *Dashed line*, mean concentration-effect curve obtained by fitting the same data with the two-site receptor occupation model as presented in legend to Fig. 8 (eq. 2), including channel block by ACh: $E = E_{max}\cdot[c_A/(1 + c_A)]^2\cdot\{1/(1 + [ACh]/IC_{50})\}$ (see Discussion). B, Concentration-effect curve of atropine for the inhibition of 1 mM ACh-induced ion current at −40 mV. Inward current amplitudes in the presence of atropine were normalized to those of control inward currents induced with 1 mM ACh. *Data points*, mean ± standard deviation values for three oocytes. *Line*, mean concentration-effect curve calculated from the parameters estimated from fitting inhibition curves according to $E = 100/\{1 + (IC_{50}/[\text{atropine}])^n\}$ to the data for the three experiments. The mean IC_{50} value and n were 4.5 μM atropine and −0.96, respectively. Dashed line, predicted by the model presented in legend to Fig. 8 (eq. 3).

predicted from the results on the voltage dependence of ion channel block (Fig. 3).

To further optimize experimental conditions with respect to potentiation, the relation between the effect of 10 μM atropine and ACh concentration was investigated at the holding potential of −40 mV. The results of these experiments (Fig. 6) show that potentiation occurs only at low agonist concentration. The 1 μM ACh-induced inward current

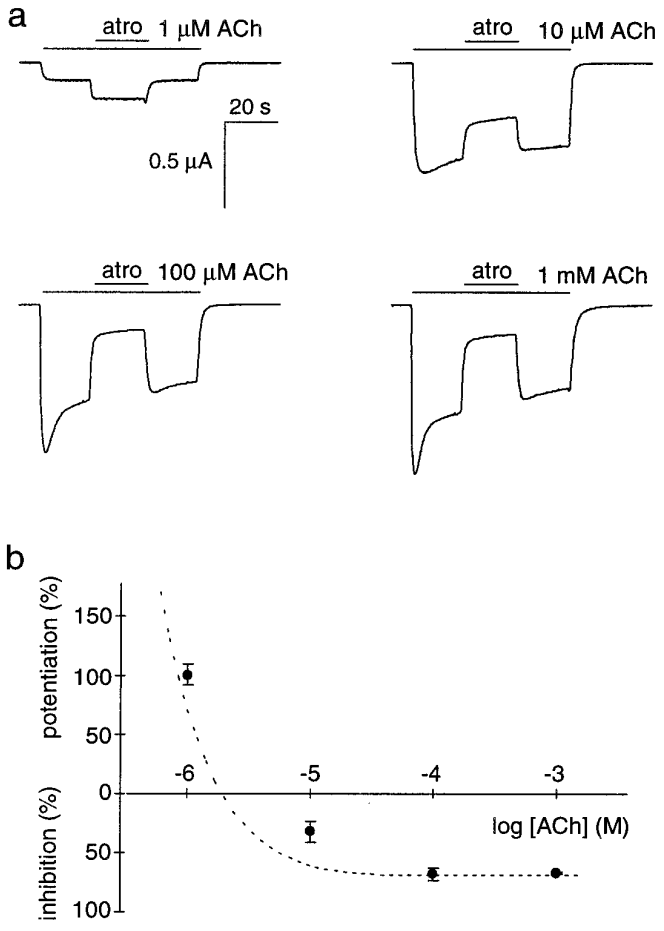

Fig. 6. Effect of agonist concentration on the balance between potentiation and inhibition of $\alpha4\beta4$ nAChR-mediated ion current by atropine. A, Effects of 10 μM atropine on ion currents evoked by 1, 10, 100, and 1000 μM ACh measured at a holding potential of -40 mV. Horizontal bars, application of ACh and atropine. Atropine potentiates the 1 μM ACh-induced inward current and inhibits the ion currents evoked by higher concentrations of the agonist. Note the absence of current transients on application and removal of atropine. Similar results were obtained from an additional two oocytes. B, Steady state effects of 10 μM atropine on 1, 10, 100, and 1000 μM ACh-induced ion currents, measured at the holding potential of -40 mV. Atropine potentiates the ACh-induced inward current only at the 1 μM ACh concentration. At ACh concentrations of $\geq$10 μM, the effect of atropine is reversed into inhibition. *Data points*, mean $\pm$ standard deviation (*bars*) values for three oocytes. At 1 mM ACh, the mean $\pm$ standard deviation is smaller than the symbol. *Dashed line*, predicted by the model presented in legend to Fig. 8 (eq. 3) (see Discussion).

was potentiated by 10 μM atropine, whereas in the same oocytes inward currents induced by 10 μM to 1 mM ACh were inhibited by 10 μM atropine. Despite the pronounced inhibitory effect of 10 μM atropine, current transients were never observed at the onset and reversal of the atropine effects during 100 μM and 1 mM ACh-induced ion currents (Fig. 6A), indicating that the potentiating effect is completely surmounted. The inhibitory effect of atropine is not surmounted, indicating that at the highest agonist concentrations the only effect of atropine remaining is noncompetitive ion channel block. The results of three oocytes shown in Fig. 6B demonstrate that the potentiating and inhibitory effects of 10 μM atropine are equal at an ACh concentration of 1–10 μM.

The relation between potentiation of $\alpha4\beta4$ nAChR-mediated current and atropine concentration has been investigated at the holding potential of -40 mV and at the ACh concentration of 1 μM, at which potentiation by atropine is optimized. The application of different concentrations of atropine during the ACh-induced inward current revealed potentiation of the ion current by atropine concentrations of up to 10 μM (Fig. 7A). However, at this concentration, inhibition by atropine became also apparent, and the inhibitory effect increased steeply at concentrations of >10 μM atropine. Steady state effects of atropine were defined as the steady current amplitude in the presence of atropine relative to the current level just before atropine application (Fig. 7B). The

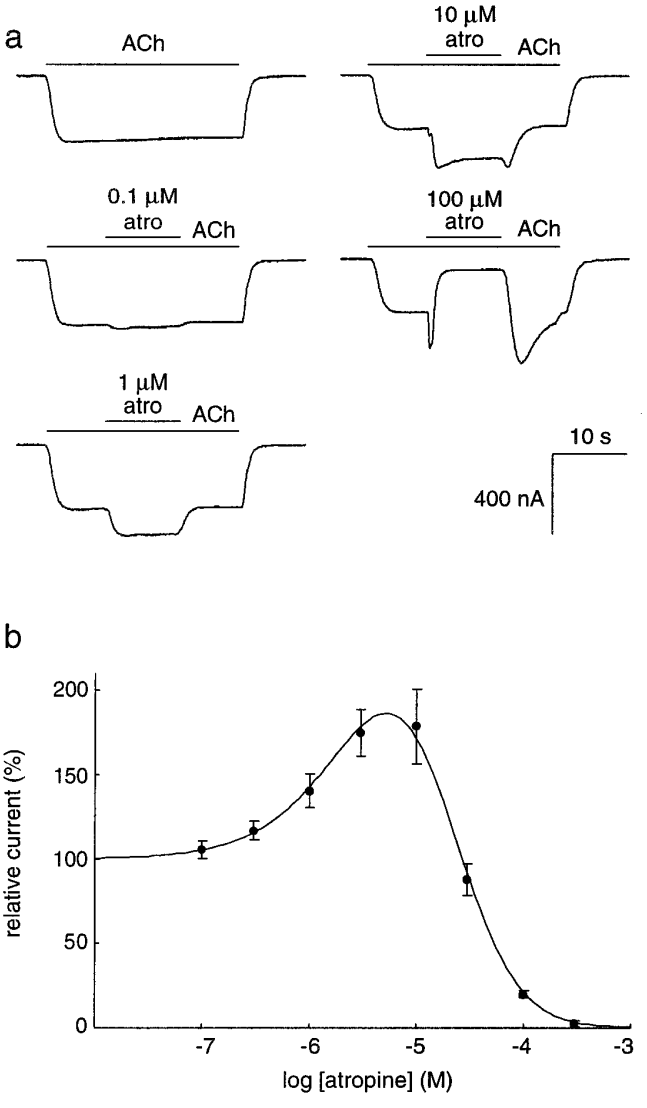

Fig. 7. Concentration dependence of atropine effects on $\alpha4\beta4$ nAChR-mediated ion currents. A, Effects of various concentrations of atropine on ion currents induced by 1 μM ACh at -40 mV holding potential. *Horizontal bars*, application of ACh and atropine. At concentrations of 0.1–3 μM, atropine potentiated the ACh-induced ion current, whereas at higher atropine concentrations, the initial potentiation was followed by inhibition of ACh-induced ion current. B, Concentration dependence of the steady state effects of atropine on $\alpha4\beta4$ nAChR-mediated ion current. Steady state effects were determined as the steady current level in the presence of atropine relative to the current level just before atropine application. Values are mean $\pm$ standard deviation for four oocytes. *Bell-shaped curve*, fit of a model combining receptor occupation and ion channel block by atropine to the data (Fig. 8, eq. 3) (Discussion).

resulting bell-shaped concentration-effect curve shows potentiation in the range of 0.3–10 μM atropine and inhibition at ≥30 μM atropine. The mechanisms to account for the potentiating and inhibitory effects of atropine are discussed.

Discussion

The results demonstrate that neuronal nAChR-mediated ion currents are modulated by the classic mAChR antagonist atropine. At hyperpolarized membrane potential and high agonist concentration, atropine always inhibits the ACh-induced inward current. The degree of this inhibition varies for the different nAChR subunit combinations but cannot be related to a specific α or β receptor subunit. At low agonist concentration, the inhibitory effect of atropine is significantly reduced for most subtypes of nAChR that we investigated, and unexpectedly, atropine potentiates ion current mediated by α4 subunit-containing nAChR (Table 1). Detailed investigation of atropine effects on the more sensitive α4β4 nAChR demonstrates that the potentiating effect differs from the inhibitory effect in being more pronounced at low agonist concentration and at depolarized membrane potential. Ion currents and indirect effects mediated by endogenous mAChRs were not observed in the present experiments. The absence of endogenous mAChRs, which has also been reported in other oocyte studies (13, 27–30), is possibly due to the collagenase treatment and defolliculation of the oocytes (20).

Inhibition. The inhibition of ion currents evoked by high concentrations of ACh in oocytes expressing the more sensitive α4β4 nAChR by atropine was found to be noncompetitive (Fig. 2B). The reduction in ion current amplitude by atropine was voltage dependent and associated with an acceleration of inward current decay and a transient tail current on removal of atropine (Figs. 3 and 4). From these results, it is concluded that the noncompetitive inhibitory effect of atropine on nAChRs is caused by the occlusion of open ion channels. IC_{50} values of atropine for blocking ion currents induced by high concentrations of ACh at −80 and −40 mV of 0.96 and 4.1 μM, respectively, are predicted on the basis of the data in Fig. 3C. These predicted values are close to the observed IC_{50} values of 0.66 μM (Fig. 2A) and 4.5 μM (Fig. 5B) atropine at the respective membrane potentials. This indicates that the noncompetitive effect of atropine is adequately accounted for by voltage-dependent ion channel block.

Table 1 shows that α4β4, α2β4, and α7 nAChRs have a similar high sensitivity to block by atropine. Other data available on the sensitivity of neuronal nAChRs to inhibition by atropine are restricted to homo-oligomeric nAChRs. The IC_{50} value of 125 μM atropine for the inhibition of human α7 nAChRs as determined from responses evoked with 30 μM nicotine at a holding potential of −60 mV (31) suggests that the human α7 is less sensitive than the rat α7 nAChR (Table 1). Reported IC_{50} values of atropine for inhibition of rat α9 nAChRs (1.3 μM; ref. 13) and of chicken α7 (7.1 μM) and α8 (0.4 μM; ref. 12) nAChRs have been obtained under conditions less favorable for ion channel block (i.e., low agonist concentrations were used at moderately hyperpolarized membrane potentials). The data in Table 1 show that the inhibitory effects of atropine are significantly reduced at low agonist concentration, except for the effect on α3β4 nAChR. This suggests that potentiation, which is clearly observed for α4β2 and α4β4 nAChR, may occur at other subtypes of nAChR as well but to a lesser degree.

Potentiation. Investigation of concentration and voltage dependence revealed that atropine causes a mixture of inhibitory and potentiating effects (Figs. 2B, 4, 6, and 7). Taking advantage of the reduced ion channel block at depolarized membrane potential (Fig. 4), experimental conditions were improved to investigate the nature of the potentiating effect. The results in Fig. 6 illustrate that the change in the balance between potentiation and inhibition is due to a reduction in the potentiating effect with increasing agonist concentration. Because inhibition is noncompetitive at high ACh concentrations (see also Fig. 2B), the saturation of the effects at ≥100 μM ACh shows that potentiation is completely surmounted at high agonist concentration. In addition, the experimental data (Figs. 2B and 5; Table 1) indicate that at a low agonist concentration, potentiation by atropine occurs at depolarized as well as at hyperpolarized membrane potentials. From these results, it is concluded that the potentiating effect depends on agonist concentration but not strongly on membrane potential. The surmountability of the potentiating effect of atropine by high concentrations of the agonist indicates that unlike the voltage-dependent inhibition, potentiation of nAChRs by atropine is a competitive effect. The distinct mechanisms of potentiation and inhibition and differences in voltage and concentration dependence of the two effects of atropine demonstrate that atropine interacts with two independent sites of the nAChR. The site associated with the noncompetitive, voltage-dependent inhibition is associated with ion channel block, and the site mediating the competitive, potentiating effect of atropine is the agonist recognition site of the nAChR. Competitive binding of atropine to neuronal nAChRs has been demonstrated previously for chicken α7 nAChR, at which atropine displaces α-bungarotoxin with an apparent affinity of 148 μM (32).

Mechanism of action of atropine and other drugs. Previously, potentiation and inhibition of nAChR-mediated ion currents in PC12 cells have been reported for the cholinesterase inhibitor 1-methyl-galanthamine (33). Like atropine, cholinesterase inhibitors inhibit nAChR-mediated ion currents by open channel block, but a noncompetitive mechanism is thought to be involved in potentiation by *1*-methyl-galanthamine as well (26, 34). The action of atropine more strongly resembles that of curare-like drugs, which also cause a combination of potentiating and inhibitory effects on nAChRs. The striking similarities between the actions of atropine and curare-like drugs are that both potentiate the nAChR-mediated ion current only in the presence of low concentrations of agonist and that neither (+)-tubocurarine (22) nor atropine (Fig. 3B) causes direct agonist effects on neuronal nAChRs expressed in *X. laevis* oocytes. However, curare-like drugs appear to be weak partial agonists on fetal, end-plate-type nAChRs expressed in quail fibroblasts (35), and (+)-tubocurarine activates unitary currents in bovine chromaffin cells (36). The presently found dependence of the potentiation by atropine on agonist concentration (Fig. 6) is consistent with models previously proposed (22, 35) in which the simultaneous occupation of one agonist recognition site with an agonist molecule and of a second agonist recognition site with the "blocking drug" induces ion channel activation. The concentration-dependent potentiation and inhibition of neuronal nAChRs by atropine (Fig. 7) have been evaluated

using the equilibrium receptor occupation model of Cachelin and Rust (22). The model assumes that (i) the neuronal nAChR contains two identical agonist recognition sites, (ii) these sites must be occupied by ACh molecules or by one ACh and one atropine molecule to produce an activatable state of the receptor, and (iii) ligand binding kinetics are rapid. The original model was extended to incorporate noncompetitive ion channel block by atropine, resulting in eight distinctly occupied states (Fig. 8). The data of Fig. 7 were closely fitted by the steady state occupation/block function derived (see legend to Fig. 8A). The apparent affinity (K_1) of ACh for the agonist recognition site was estimated by fitting a model for two-site receptor occupation and ion channel block by ACh to the concentration-effect data in Fig. 5A (*dashed line*). The mean of the estimated K_1 values as 16.9 ± 9.4 μM (three oocytes). The K_1 value of 16.9 μM ACh and the K_b value of 4.5 μM for noncompetitive channel block at −40 mV by atropine (Fig. 5B) were entered in the model as constants, and the apparent affinity of atropine for the agonist recognition site (K_2) and the efficacy factor f were estimated by nonlinear regression. The values obtained for K_2 and f were 29.9 ± 0.7 μM and 0.75 ± 0.09, respectively. Subsequently, all these parameter estimates were used to simulate the results obtained in Figs. 5B and 6B (*dashed lines*). With the same set of estimated parameters, the effects of ACh concentration on the concentration-effect curve of atropine were also simulated by the model. This simulation clearly demonstrates the bell-shaped potentiation/inhibition curves at low concentrations of ACh and atropine and the monophasic inhibition curves at higher concentrations of ACh (Fig. 8B).

The various effects of atropine on nAChR-mediated ion current are accounted for by the equilibrium receptor occupation model combined with ion channel block. The difference in the affinities of atropine for the agonist recognition site (K_2 = 29.9 μM) and ion channel block (K_b = 4.5 μM) indicates that channel block by atropine will always be the predominant inhibitory effect at membrane potentials more negative than −40 mV. In the presence of an excess of ACh, atropine will cause ion channel block only (AAR^B; see legend to Fig. 8). This is consistent with the low IC_{50} value of atropine and the moderate slope of the inhibition curves obtained at high concentrations of ACh (Figs. 2A and 5B) compared with the higher IC_{50} value of atropine and the steep slope of inhibition of 1 μM ACh-induced current (Fig. 7B). These features are also predicted by the model illustrated in Fig. 8B.

General implications of the findings. The sensitivity of various subtypes of neuronal nAChRs to atropine complicates the interpretation of results obtained in many studies of neuronal nAChRs expressed in oocytes, in which micromolar concentrations of atropine were routinely added to the extracellular solutions to block putative endogenous mAChRs (see Fig. 2B). Results of studies of more complex systems, such as brain slices, in which atropine is used as a tool to discriminate between mAChR- and nAChR-mediated effects should also be treated with caution. Adverse potentiating or inhibitory effects may be more or less pronounced depending on nAChR subtype, cell membrane potential, and agonist concentration. Because mAChRs have affinities to atropine that are several orders of magnitude higher (7) than those of the more sensitive subtypes of nAChR, low therapeutic doses of atropine should not interfere with nAChR function. However, whether potentiating effects of atropine on neuronal nAChRs in the central nervous system are involved in the excitatory symptoms associated with overt toxic

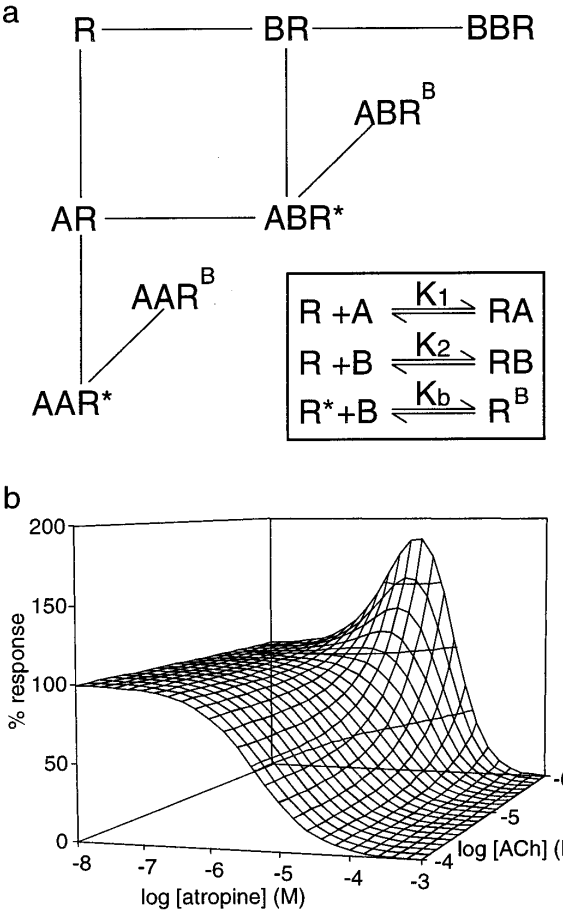

Fig. 8. A, Eight-state model to explain the equilibrium effects of atropine on ACh-induced ion current mediated by the α4β4 nAChR (modified after Ref. 22). *R*, free receptor; *A*, ACh; *B*, atropine. Occupation of two agonist recognition sites by ACh (AAR*) as well as occupation of one site by ACh and a second site by atropine (ABR*) result in activated receptor states. The conformational change from the activated states (*) to the open states is omitted. Occupation of all agonist recognition sites by atropine (BBR) does not lead to an activated receptor, and open ion channels may be blocked by atropine (AAR^B and ABR^B). The ion current amplitude as a function of steady state occupancy of the AAR* and ABR* states combined with ion channel block is described by $I(x_A,x_B) \approx [(c_A^2 + 2fc_Ac_B)/(1 + c_A + c_B)^2]\cdot[1/(1 + x_B/K_b)]$ (*inset, first equation*). The function is equivalent to the bell-shaped concentration-effect curve previously used to model the effects of (+)-tubocurarine (see eq. 5 in Ref. 22) multiplied by a single-site inhibition curve. x_A and x_B, ACh and atropine concentration, respectively; c_A and c_B, normalized ACh and atropine concentrations x_A/K_1 and x_B/K_2, respectively; f, factor to account for a difference in efficacy of ACh and atropine; K_b, apparent affinity of atropine for ion channel block. In addition, control ion current in the absence of atropine is described by $I(x_A,0) = [c_A/(1 + c_A)]^2$ (*inset, second equation*). Because each response is expressed as a percentage of the control response, the first equation is multiplied by 100 and divided through $I(x_A,0)$ to yield the normalized response amplitude: $I(x_A,x_B) = 100\cdot\{[(1 + c_A)/c_A]^2\cdot[(c_A^2 + 2fc_Ac_B)/(1 + c_A + c_B)^2]\}\cdot[1/(1 + x_B/K_b)]$ (*inset, third equation*). B, Modeling of atropine effects dependent on ACh concentration; parameters used to generate the concentration-effect surface are obtained from data in Figs. 5 and 7. Three contours, 50%, 100%, and 150% response. The model accounts for the potentiating effect of low concentrations of atropine at low ACh concentrations only and demonstrates a leftward shift of the IC_{50} value of atropine with increasing ACh concentration.

doses of atropine (37) remains to be determined. At concentrations as low as 0.1 μM, which are frequently used in experiments to antagonize mAChRs, direct effects of atropine on the functioning of several subtypes of neuronal nAChRs cannot be ignored.

Acknowledgments

We thank Dr. Jim Patrick (Baylor College of Medicine, Houston, TX) for donating the cDNA clones of nAChR subunits, Jenny Narraway and Kees Koster (Hubrecht Laboratory, Utrecht, The Netherlands) for supplying the *X. laevis* oocytes, Ing. Aart de Groot for excellent technical assistance, Dr. Johannes van Hooft for critically reading and commenting on the manuscript, and Dr. Sjeng Horbach for molecular biological support.

References

1. Dale, H. H. The action of certain esters and ethers of choline and their relation to muscarine. *J. Pharmacol. Exp. Ther.* **6:**147–190 (1914).
2. Koelle, G. B. Acetylcholine, in *Encyclopedia of Neuroscience, Vol. I.* (G. Adelman, ed.). Birkhauser, Boston/Basel/Stuttgart, 1–2 (1987).
3. Changeux, J. P. Acetylcholine receptor, in *Encyclopedia of Neuroscience, Vol. I.* (G. Adelman, ed.). Birkhauser, Boston/Basel/Stuttgart, 2–3 (1987).
4. Bonner, T. I., A. C. Young, M. R. Brann, and N. J. Buckley. Identification of a family of muscarinic acetylcholine receptor genes. *Science (Washington D. C.)* **237:**527–532 (1987).
5. Hosey, M. M. Diversity of structure, signalling and regulation within the family of muscarinic cholinergic receptors. *FASEB J.* **6:**845–852 (1992).
6. Sargent, P. B. The diversity of neuronal nicotinic acetylcholine receptors. *Annu. Rev. Neurosci.* **16:**403–443 (1993).
7. Richards, M. H. Pharmacology and second messenger interactions of cloned muscarinic receptors. *Biochem. Pharmacol.* **42:**1645–1653 (1991).
8. Adler, M., E. X. Albuquerque, and F. J. Lebeda. Kinetic analysis of endplate currents altered by atropine and scopolamine. *Mol. Pharmacol.* **14:** 514–529 (1978).
9. Connor, E. A., S. M. Levy, and R. L. Parsons. Kinetic analysis of atropine-induced alterations in bullfrog ganglionic fast synaptic currents. *J. Physiol. (Lond.)* **337:**137–158 (1983).
10. Feltz, A., W. A. Large, and A. Trautmann. Analysis of atropine action at the frog neuromuscular junction. *J. Physiol. (Lond.)* **269:**109–130 (1977).
11. McGehee, D. S., and L. W. Role. Physiological diversity of nicotinic acetylcholine receptors expressed by vertebrate neurons. *Annu. Rev. Physiol.* **57:**521–546 (1995).
12. Gerzanich, V., R. Anand, and J. Lindstrom. Homomers of α8 and α7 subunits of nicotinic receptors exhibit similar channel but contrasting binding site properties. *Mol. Pharmacol.* **45:**212–220 (1994).
13. Elgoyhen, A. B., D. S. Johnson, J. Boulter, D. E. Vetter, and S. F. Heinemann. α9: an acetylcholine receptor with novel pharmacological properties expressed in rat cochlear hair cells. *Cell* **79:**705–715 (1994).
14. Fan, P., and F. F. Weight. The effect of atropine on the activation of 5-hydroxytryptamine$_3$ channels in rat nodose ganglion neurons. *Neuroscience* **62:**1287–1292 (1994).
15. Deneris, E. S., J. Connolly, S. W. Rogers, and R. Duvoisin. Pharmacological and functional diversity of neuronal nicotinic acetylcholine receptors. *Trends Pharmacol. Sci.* **12:**34–40 (1991).
16. Zwart, R., and H. P. M. Vijverberg. Atropine inhibits neuronal nicotinic receptors. *Soc. Neurosci. Abstr.* **22:**1522 (1996).
17. Stühmer, W. Electrophysiological recording from *Xenopus* oocytes. *Methods Enzymol.* **207:**319–339 (1992).
18. Marquardt, D. W. An algorithm for least-squares estimation of nonlinear parameters. *J. Soc. Indust. Appl. Math.* **11:**431–441 (1963).
19. Kusano, K., R. Miledi, and J. Stinnakre. Cholinergic and catecholaminergic receptors in the *Xenopus* oocyte membrane. *J. Physiol. (Lond.)* **328:** 143–170 (1982).
20. Dascal, N., E. M. Landau, and Y. Lass. *Xenopus* oocytes resting potential, muscarinic responses and the role of calcium and guanosine 3′,5′-cyclic monophosphate. *J. Physiol. (Lond.)* **352:**551–574 (1984).
21. Oortgiesen, M., and H. P. M. Vijverberg. Properties of neuronal type acetylcholine receptors in voltage clamped mouse neuroblastoma cells. *Neuroscience* **31:**169–179 (1989).
22. Cachelin, A. B., and G. Rust. Unusual pharmacology of (+)-tubocurarine with rat neuronal nicotinic acetylcholine receptors containing β4 subunits. *Mol. Pharmacol.* **46:**1168–1174 (1994).
23. Garcia-Colunga, J., and R. Miledi. Effects of serotonergic agents on neuronal nicotinic acetylcholine receptors. *Proc. Natl. Acad. Sci. USA* **92:** 2919–2923 (1995).
24. Lester, R. A. J., and J. A. Dani. Acetylcholine receptor desensitization induced by nicotine in rat medial habenula neurons. *J. Neurophysiol.* **74:**195–206 (1995).
25. Zwart, R., M. Oortgiesen, and H. P. M. Vijverberg. Differential modulation of $\alpha3\beta2$ and $\alpha3\beta4$ neuronal nicotinic receptors expressed in *Xenopus* oocytes by flufenamic acid and niflumic acid. *J. Neurosci.* **15:**2168–2178 (1995).
26. Bufler, J., C. Franke, H. Parnas, and J. Dudel. Open channel block by physostigmine and procaine in embryonic-like nicotinic receptors of mouse muscle. *Eur. J. Neurosci.* **8:**677–687 (1996).
27. Sugiyama, H., Y. Hisanaga, and C. Hirono. Induction of muscarinic cholinergic responsiveness in *Xenopus* oocytes by mRNA isolated from rat brain. *Brain Res.* **338:**346–350 (1985).
28. Kubo, T., K. Fukada, A. Mikami, A. Maeda, H. Takahashi, M. Mishina, T. Haga, K. Haga, A. Ichiyama, K. Kangawa, M. Kojima, M. Matsuo, H. Hirose, and S. Numa. Cloning, sequencing and expression of complementary DNA encoding the muscarinic acetylcholine receptor. *Nature (Lond.)* **323:**411–416 (1986).
29. Kullberg, R., J. L. Owens, P. Camacho, G. Mandel, and P. Brehm. Multiple conductance classes of mouse nicotinic acetylcholine receptors expressed in *Xenopus* oocytes. *Proc. Natl. Acad. Sci. USA* **87:**2067–2071 (1990).
30. Cohen, B. N., A. Figl, M. W. Quick, C. Labarca, N. Davidson, and H. A. Lester. Regions of $\beta2$ and $\beta4$ responsible for differences between the steady state dose-response relationships of the $\alpha3\beta2$ and $\alpha3\beta4$ neuronal nicotinic receptors. *J. Gen. Physiol.* **105:**745–764 (1995).
31. Peng, X., M. Katz, V. Gerzanich, R. Anand, and J. Lindstrom. Human α7 acetylcholine receptor: cloning of the α7 subunit from the SH-SY5Y cell line and determination of pharmacological properties of native receptors and functional α7 homomers expressed in *Xenopus* oocytes. *Mol. Pharmacol.* **45:**546–554 (1994).
32. Anand, R., X. Peng, and J. Lindstrom. Homomeric and native α7 acetylcholine receptors exhibit remarkably similar but non-identical pharmacological properties, suggesting that the native receptor is a heteromeric protein complex. *FEBS Lett.* **327:**241–246 (1993).
33. Schrattenholz, A., E. F. R. Pereira, U. Roth, K. H. Weber, E. X. Albuquerque, and A. Maelicke. Agonist responses of neuronal nicotinic acetylcholine receptors are potentiated by a novel class of allosterically acting ligands. *Mol. Pharmacol.* **49:**1–6 (1996).
34. Pereira, E. F. R., S. Reinhardt-Maelicke, A. Schrattenholz, A. Maelicke, and E. X. Albuquerque. Identification and functional characterization of a new agonist site on nicotinic acetylcholine receptors of cultured hippocampal neurons. *J. Pharmacol. Exp. Ther.* **265:**1474–1491 (1993).
35. Fletcher, G. H., and J. H. Steinbach. Ability of nondepolarizing neuromuscular blocking drugs to act as partial agonists at fetal and adult mouse muscle nicotinic receptors. *Mol. Pharmacol.* **49:**938–947 (1996).
36. Nooney, J. M., J. A. Peters, and J. J. Lambert. A patch clamp study of the nicotinic acetylcholine receptor of bovine adrenomedullary chromaffin cells in culture. *J. Physiol. (Lond.)* **455:**503–527 (1992).
37. Weiner, N. Atropine, scopolamine, and related antimuscarinic drugs, in *The Pharmacological Basis of Therapeutics* (A. Goodman-Gilman, L. S. Goodman, T. W. Rall, and R. Murad, eds.). Pergamon Press, New York, 130–144 (1985).

Send reprint requests to: Dr. Ruud Zwart, Research Institute of Toxicology, Utrecht University, P.O. Box 80.176, NL-3508 TD Utrecht, The Netherlands. E-mail: r.zwart@ritox.dgk.ruu.nl